

# Experimental detection and focusing in shallow water by decomposition of the time reversal operator

Claire Prada,<sup>a)</sup> Julien de Rosny, Dominique Clorennec, Jean-Gabriel Minonzio, Alexandre Aubry, and Mathias Fink

*Laboratoire Ondes et Acoustique, ESPCI, 75005 Paris, France*

Lothar Berniere, Philippe Billand, Sidonie Hibrat, and Thomas Folegot<sup>b)</sup>

*Atlantide, Technopole Brest Iroise, 29200 Brest, France*

(Received 27 October 2006; revised 14 May 2007; accepted 18 May 2007)

A rigid 24-element source-receiver array in the 10–15 kHz frequency band, connected to a programmable electronic system, was deployed in the Bay of Brest during spring 2005. In this 10- to 18-m-deep environment, backscattered data from submerged targets were recorded. Successful detection and focusing experiments in very shallow water using the decomposition of the time reversal operator (DORT method) are shown. The ability of the DORT method to separate the echo of a target from reverberation as well as the echo from two different targets at 250 m is shown. An example of active focusing within the waveguide using the first invariant of the time reversal operator is presented, showing the enhanced focusing capability. Furthermore, the localization of the scatterers in the water column is obtained using a range-dependent acoustic model.

© 2007 Acoustical Society of America. [DOI: 10.1121/1.2749442]

PACS number(s): 43.30.Gv, 43.30.Vh, 43.60.Tj [DRD]

Pages: 761–768

## I. INTRODUCTION

Time reversal focusing in a waveguide using a source receiver array (SRA) was demonstrated in an ultrasound experiment (Fink, 1997). Taking advantage of the multiple reflections at the waveguide interfaces, time reversal allows high resolution focusing. This property was proven by several underwater time reversal experiments starting with the one by Kuperman and his team (Kuperman *et al.*, 1998). Then, the strong potential of time reversal techniques for underwater communication in shallow water was demonstrated (Edelmann *et al.*, 2002). High resolution offered by time reversal has also been exploited for detection and separation of scatterers in an ultrasonic waveguide using the decomposition of the time reversal operator (DORT method). This method is a scattering analysis technique derived from the study of the iterative time reversal process (Prada and Fink, 1994). It was applied in an ultrasonic water waveguide with a flat rigid bottom, demonstrating multitarget detection and selective focusing with high resolution. The resolution of this method was used to separate the signal reflected by two close scatterers and then focus selectively at any of them (Mordant *et al.*, 1999). It was then the object of several studies for ocean applications (Lingevitch *et al.*, 2002; Yokoyama *et al.*, 2001). Its ability to separate the echo of a target from bottom reverberation was shown in a laboratory experiment (Folegot *et al.*, 2003).

Recently, the DORT method has been tested at sea with a vertical SRA and using an echo repeater to simulate the target response (Gaumont *et al.*, 2006). The signal transmitted back to the SRA provided by an echo repeater offers

much higher signal to noise ratio than a passive target but, unfortunately was free of bottom reverberation. In addition, the SRA was mounted to a small vessel that heaved significantly due to wave motion, which induced serious loss of coherence that affects the technique. Another recent paper (Sabra *et al.*, 2006) proposes to use the time reversal technique to enhance focusing on a target located on the bottom in presence of reverberation. A reflectivity map from the measured array response matrix is built, using passive (i.e., numerical) iterative time reversal. This method allowed successful detection of an ensemble of 12 spheres of diameter 50 cm on the bottom using a 96 element billboard array of central frequency 3.5 kHz, in 50 m water depth at range 200 m.

The present paper focuses on the application of the DORT method to detection in very shallow water in the presence of strong reverberation. A rigid vertical SRA with fully programmable parallel processed generators has been developed in the 10–15 kHz frequency band. After initial tests in a pool basin (Clorennec *et al.*, 2005; Folegot *et al.*, 2005), the system was deployed in the Bay of Brest for sea trials during spring 2005. Backscattered data from small submerged targets have been recorded for distances up to 600 m in a water depth varying from 10 to 18 m and the DORT method was applied for detection and localization of these targets. Furthermore, focusing was achieved either by time reversal or by transmission of the first eigenvector of the time reversal operator.

The system and the experimental setup are described in Sec. II. The signal measurement and analysis technique are developed in Sec. III. Several results from two different experiments are presented in Secs. IV and V. The first one is a detection experiment with two targets at the same range but different depth, showing the ability to separate the echo of

<sup>a)</sup>Electronic mail: claire.prada-julia@espci.fr

<sup>b)</sup>Currently at NURC, La Spezia, Italy.



FIG. 1. The pier of Sainte Anne du Portzic in the vicinity of Brest (France) where the system was deployed. The white lines show the insonified zone.

each target. The second one shows the ability to separate the echo of a target from bottom reverberation and compares the focusing obtained by active time reversal or by transmission of the first eigenvector of the time reversal operator.

## II. EXPERIMENTAL SETUP

The experiments took place during spring 2005 in the Bay of Saint Anne du Portzic in France, a shallow water inlet (Fig. 1). This site is characterized by a significant spatial variability of the bottom interface, a rocky coastline generating strong reverberation and strong tidal currents (up to 4 knots, i.e. 2 m/s). The bathymetry has been recorded using multibeam sonar (Fig. 2). The sound speed  $c$  was measured with a profiling sound velocimeter at several distances in the whole water column and was constant at 1495 m/s. The SRA is deployed from a pier in a water depth varying from 7 to 12 m depending on tide (Fig. 3). It consists of a rigid support frame carrying 24 source/receiver transducers oper-

ating in the 10–15 kHz frequency band with a maximum source level of 203 dB re 1  $\mu$ Pa at 1 m each. The vertical transducer positions are adjustable, with a maximum array aperture of 12 m. In this experiment, they were equally spaced with a total aperture  $D=9.4$  m. Each of the 24 channels is individually controlled and amplified during transmission and reception. In addition, a 16 element flexible vertical receiver array (VRA) can be deployed from a small vessel in order to sample the acoustic field produced by the SRA. As described in Folegot *et al.* (2005), communication and synchronization between the two arrays is established via a wireless local area network. In the experiments shown here, the targets are trihedral corner acoustic retroreflectors (TCAR) consisting of three mutually perpendicular intersecting plates made of air filled honeycomb composite (Fig. 4). These targets are small, easy to handle from a small ship and moor with an anchor. The biggest target has maximum dimension 60 cm  $\approx 5\lambda$  and the smallest 40 cm.

## III. DATA ACQUISITION AND ANALYSIS

The principle of the DORT method is described in several papers (Mordant *et al.*, 1999; Prada and Fink, 1994). It requires the measurement of the array response function  $\mathbf{K}(t)$  made of the  $N \times N$  interelement impulse responses of the array ( $N=24$  in the experiment). Then, the invariants of the time reversal operator are calculated using the singular value decomposition (SVD) of the frequency response matrix  $\mathbf{K}(\omega)$ .

### A. Measurement of the array response matrix

The array response matrix  $\mathbf{K}(t)$  is measured using linear frequency modulated (LFM) sweeps transmitted from the SRA. In order to get a sufficient signal to noise ratio (SNR), the array response matrix is acquired using the Hadamard basis as proposed in Lingeitch *et al.* (2002). Such a basis is

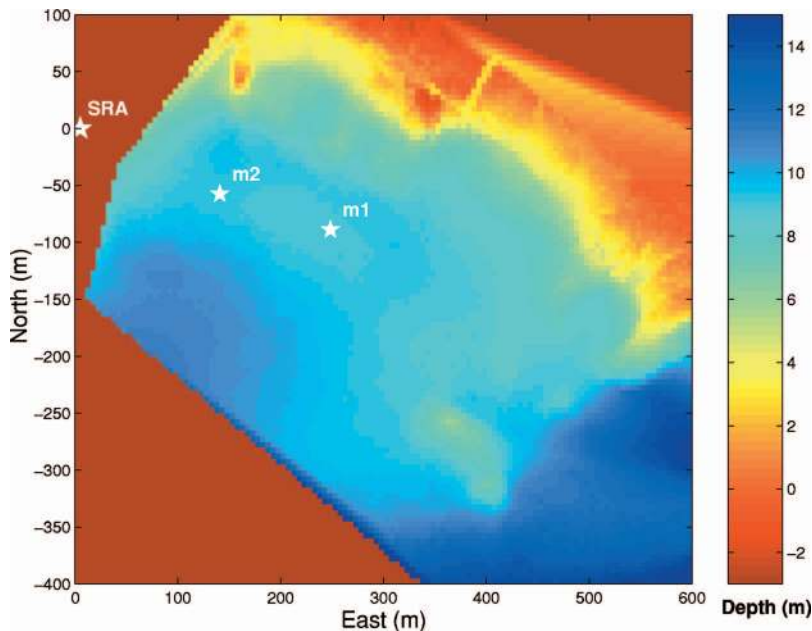


FIG. 2. Bathymetry of the bay of Sainte Anne du Portzic. The array was deployed at coordinates (0,0). The targets were successively deployed at points  $m1$  and  $m2$ .

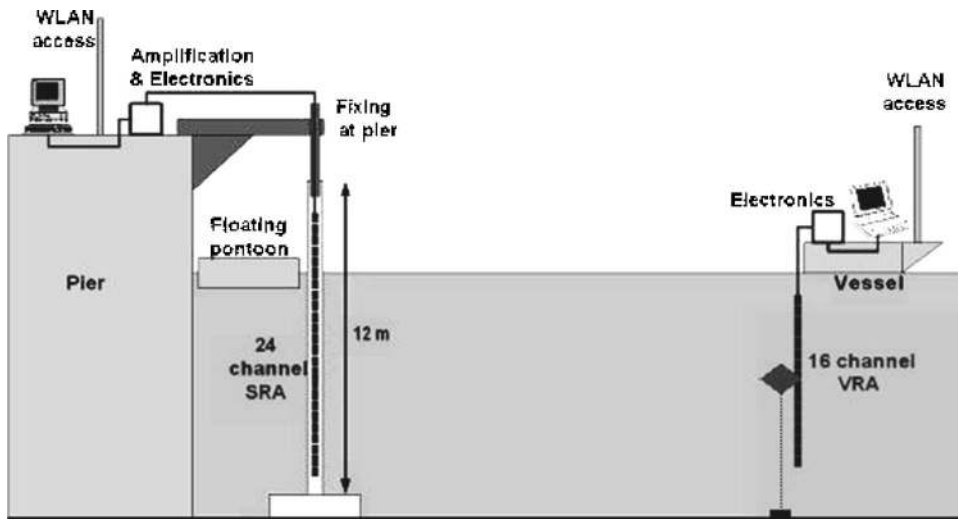


FIG. 3. Experimental setup. The SRA is deployed from a pier. The VRA is deployed from a small pleasure boat.

defined for  $N=24$  and the SNR is improved by a factor  $\sqrt{N} \approx 5$ . Then, the  $N^2$  received signals are correlated by the transmitted LFM, ensuring optimal SNR.

### B. Analysis of the array response matrix

As the reverberation leads to significant backscattered signals, the array response matrix is built from short time windows. More precisely, the matrix  $\mathbf{K}(r_0, \omega)$  is the Fourier transform of  $\mathbf{K}(t)$  between time  $t_0$  and  $t_0 + \Delta t$ , where  $t_0$  is related to the detection range  $r_0$  through the equation  $t_0 = 2r_0/c$  ( $c$  being the sound velocity) and  $\Delta t$  the window length. Due to the directivity of the transducer that is  $40^\circ$  in azimuth, and due to the unevenness of the bottom, the reverberation is very large, thus short time windows were used. A  $\Delta t = 3$  ms window was found to be a good compromise to include the complete response of one target and minimize the effects of reverberation.

The singular value decomposition of  $\mathbf{K}(r_0, \omega)$  is done for regularly shifted time windows and the singular values are presented as a function of range  $r_0$ . An increase of the singular values at a given range corresponds to an increase in the backscattered energy, which can be associated with either a discontinuity of the bottom (a rock or a slope change), or the presence of targets. This can be elucidated by exploiting the corresponding singular vectors.

### C. Backpropagation of singular vectors in free space

Singular vectors are numerically backpropagated to determine whether they correspond to a given target or the bottom reverberation. As the medium is complex and the wavelength ( $\approx 12$  cm) is rather short, the simplest way to backpropagate the data is to assume free space propagation. For the current point  $(r_0, h)$ , the propagation vector in free space is defined as

$$\mathbf{H}(r_0, h, \omega) = \left( \frac{e^{-ikr_1}}{r_1}, \frac{e^{-ikr_2}}{r_2}, \dots, \frac{e^{-ikr_N}}{r_N} \right)$$

where  $k$  is the wave number and  $r_j = \sqrt{r_0^2 + (h - h_j)^2}$  is the distance between the  $j$ th transducer of height  $h_j$  and the point  $(r_0, h)$ . Then, for a given singular vector  $\mathbf{V}(r_0, \omega)$  of the ma-

trix  $\mathbf{K}(r_0, \omega)$ , the backpropagated field at point  $(r_0, h)$  is the scalar product of the singular vector by the propagation vector. The image  $C(r_0, h)$  is then obtained by averaging the absolute values of the field over frequencies between 11 and 14 kHz:

$$C(r_0, h) = \sum_{\omega} |\langle \mathbf{V}(r_0, \omega), \mathbf{H}(r_0, h, \omega) \rangle|.$$

The resulting image is very interesting if the free space diffraction spot size ( $\lambda r_0/D$ ) is smaller than half the water depth. For instance, with an array aperture  $D=9$  m, a wavelength  $\lambda=0.12$  and a 15 m water depth, the method can be used for distances  $r_0$  up to 600 m. We shall see from several examples that a singular vector associated with a given target

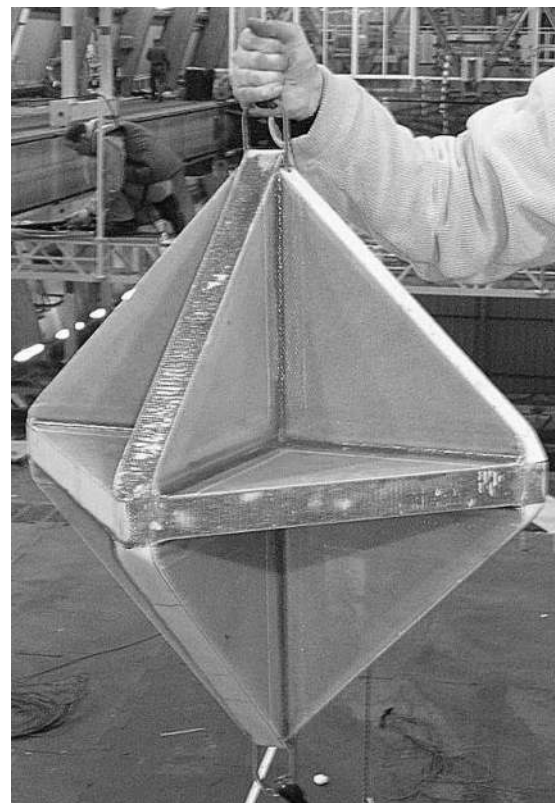


FIG. 4. The trihedral corner acoustic retroreflector.

will produce focusing on the target, plus focusing on each of the repeated images of the target with respect to the interfaces of the waveguide.

This type of backpropagation is simple as it only requires the knowledge of the array geometry and the sound velocity in water. The resulting image is unusual, but it provides a lot of information in a rapid manner. The water-air interface being flat compared to the bottom, the image with respect to this interface is generally very well defined, while images with respect to the bottom and higher order images are often more spread out. Besides, this free space backpropagation does not benefit from the guided propagation to increase resolution, that is why the backpropagation was achieved taking into account the water channel geometry as described in the next paragraph.

#### D. Backpropagation of singular vectors using a model of the waveguide

To account for guided propagation and achieve high resolution focusing, a second type of backpropagation is performed using the range-dependent acoustic model (RAM) (Collins and Westwood, 1991). RAM is based on the parabolic approximation and assumes an axisymmetric medium. As the bathymetry depends on azimuth, the bottom profile in the direction of the target is taken from the bathymetry map (Fig. 2) using an estimate of the target's position that was measured with a GPS. Besides, as the bathymetry map only starts 60 m away from the array, a linear bottom profile is assumed for the first 60 m. At last, as the transducers are mounted on a heavy rigid structure, several floats are regularly distributed along the array to reduce the weight. At low tide, part of the array is above the surface producing greater constraints. It results in a variation of the array tilt from  $2^\circ$  to  $3^\circ$  depending on tide. This angle is taken into account in the model.

In order to observe the quality of the focusing both in depth and range, the experimental singular vector is numerically backpropagated from the array. The field is displayed in the whole water column from the array to the target range. The operation differs from the free space backpropagation where the field at a given range  $r_0$  corresponds to the singular vector of  $\mathbf{K}_{r_0}$ .

The aforementioned processing does not exploit the fully programmable generators. Active focusing was also achieved using either simple time reversal or transmission of particular singular vectors. In the following, two experiments are presented showing detection, localization and then active focusing.

#### IV. FIRST EXPERIMENT: DETECTION AND SEPARATION OF TWO TARGETS

In this experiment, two TCAR are used. Both TCAR are placed at approximately 250 m from the SRA at 5.5 and 8.5 m from the bottom (point  $m1$  in Fig. 2). Thus, the targets are at about  $2500 \lambda$  from the array and in a water depth about  $100 \lambda$ . At the target distance, the free space diffraction spot is about 3.4 m, so that they are not very well resolved. In order

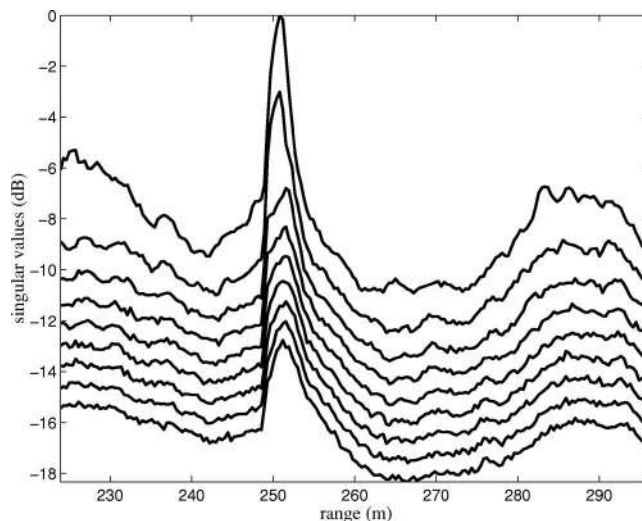


FIG. 5. Two targets at 253 m: Experimental singular values of  $\mathbf{K}_{r_0}$  calculated for a sliding 3 ms time window.

to measure the array response matrix  $\mathbf{K}(t)$ , 200-ms-long LFM sweeps are transmitted from the SRA using the Hadamard basis.

#### A. Decomposition of the array response matrix

For the analysis, a  $\Delta T=3$  ms time window is shifted by 0.5 ms steps. For each distance  $r_0$ , the matrices  $\mathbf{K}_{r_0}$  are calculated at equally spaced frequencies from 11 to 14 kHz. After SVD, the singular values are averaged over frequencies and normalized. They are presented as a function of distance from 220 to 300 m (Fig. 5). It appears that two singular values emerge at  $r_0=253$  m, the first is about 6 dB (the second about 4 dB) above reverberation singular values. For this distance, the two dominant singular values are clearly separated from the others in the whole frequency band from 10 to 15 kHz (Fig. 6). To determine the information contained in the dominant singular vectors, they are backpropagated in free space at the distance of the targets (Fig. 7). The first vector focuses at about 9 m from the bottom and the second at 6 m from the bottom, which are close to the targets

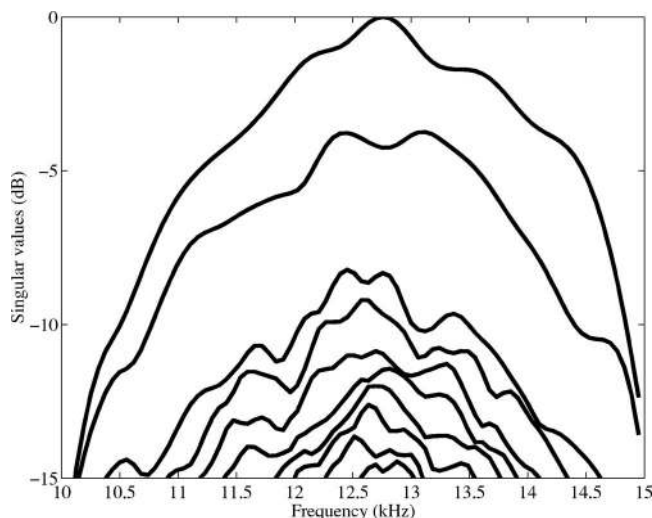


FIG. 6. Two targets at 253 m: Experimental singular values at  $r_0=253$  m, as a function of frequency. Two singular values are clearly above the others.

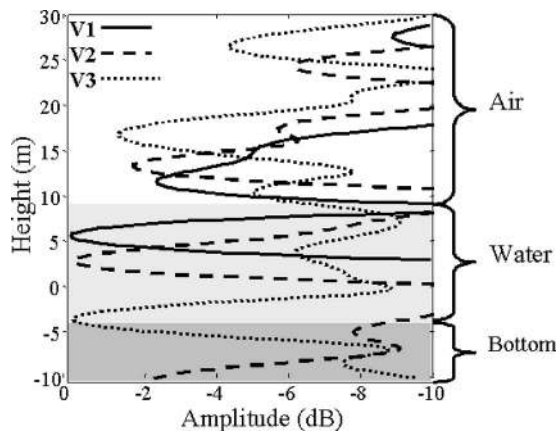


FIG. 7. Two targets at 253 m: Numerical backpropagation of the three first experimental singular vectors calculated for  $r_0=253$  m. The two first vectors focus on the two targets. The third singular vector focuses at the bottom. Height 0 m corresponds to the sea floor at the position of the SRA.

positions. The third singular vector is also backpropagated and focuses at the bottom, which is about 4 m below the antenna foot at this range. This is in agreement with the water tank experiment shown in Folegot *et al.* (2003).

In the absence of a target, information on the bottom can be found on the backpropagation in free space of the first and second singular vectors (Fig. 8). These images provide the location of the target, along with an average bottom profile. For time windows before or after the target echo, the singular vectors correspond to reverberation and focus at the bottom and at its images with respect to the interfaces. In particular, the increase in the singular values around 230 m and between 280 and 290 m can be definitely attributed to bottom reverberation. The range resolution of these images is limited by the time window length  $\Delta t=3$  ms and the LFM bandwidth, leading to about 3.5 m axial resolution. This resolution limitation is also observed on the singular values (Fig. 5).

## B. Backpropagation using RAM

The backpropagation of the first and second singular vectors corresponding to the targets are calculated for several frequencies using RAM and then averaged. The SRA tilt is taken equal to  $3.2^\circ$  and the water depth at the array equal to 8.6 m. The focusing is clearly achieved on each target with a very good resolution in depth (Fig. 9). In order to appraise the quality of the focusing, the comparison between the backpropagation in free space and with RAM code at the distance of the targets is displayed in Fig. 10. For each singular vector, the two types of propagation focus at the same depth, the improvement in resolution at  $-6$  dB is about 3.5, which means that at least one bottom and one surface reflection contribute to the reconstruction with RAM. A better knowledge of the water channel and the use of a three-dimensional code would certainly result in even better resolution.

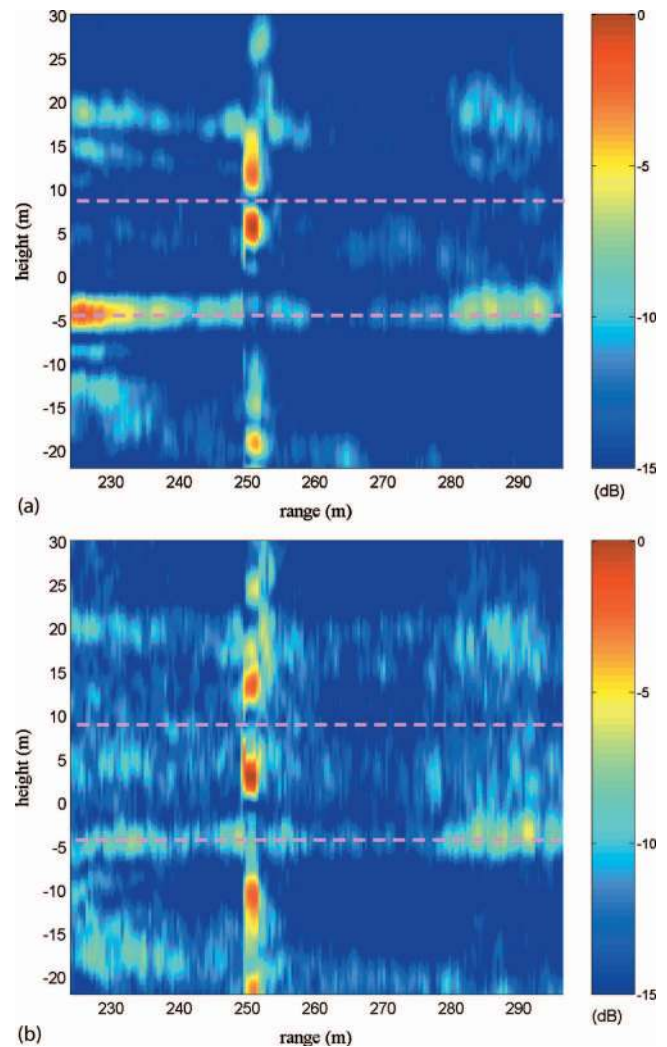


FIG. 8. Two targets at 253 m: Numerical backpropagation in free space of the first (a) and second (b) experimental singular vectors obtained for shifted time windows. The pink dashed lines indicate the bottom and the surface. The color scale is in decibels. Height 0 corresponds to the antenna foot.

## V. SECOND EXPERIMENT: ACTIVE FOCUSING ON A SINGLE TARGET

In the second experiment, the TCAR is placed approximately at 140 m from the array and at 7 m from the bottom (point  $m_2$  in Fig. 2). The purpose is to compare simple active time reversal of the target echo with the active transmission of a singular vector. The vertical receiver array is deployed at the position of the target to sample the acoustic field. This relatively short distance was chosen to avoid the strong tide current that renders measurement on the VRA difficult for longer distances. The water depth at the array position is 10 m so that all the elements are immersed. As in the first experiment, the array response matrix is acquired using the Hadamard basis and 150 ms frequency sweeps.

### A. Time reversal and DORT analysis

The array response matrices are calculated for sliding 3 ms time windows. The singular value decomposition of each matrix is then achieved. For comparison with the singular values, the energy of the echo after broadside transmission is also calculated for the same set of time windows.

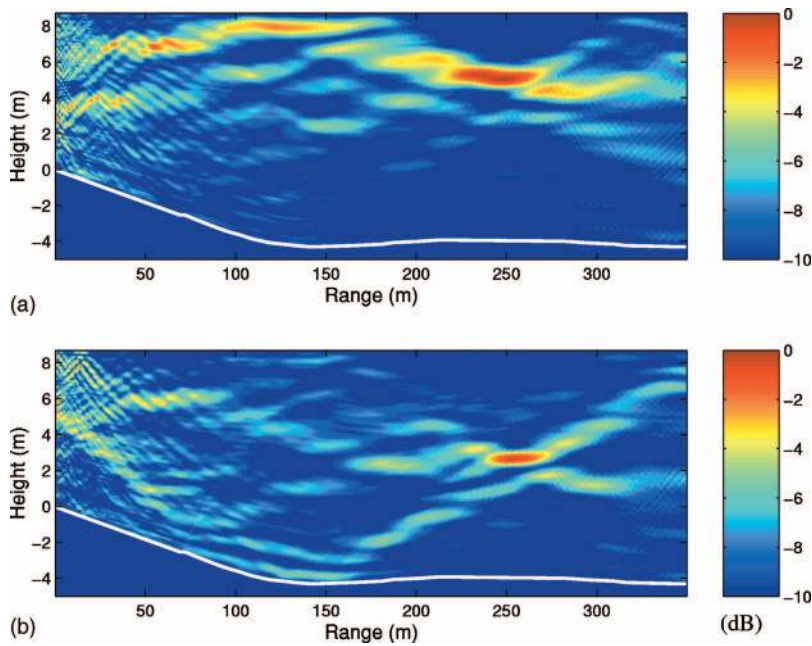


FIG. 9. Two targets at 253 m: Average field obtained by RAM backpropagation of the first (a) and second (b) experimental singular vectors calculated on the same time window as in Fig. 7, i.e.,  $r_0=253$  m.

Broadside transmission corresponds to the transmission of the first Hadamard vector (all elements transmit the same LFM simultaneously). The echo received on the  $N$  transducers are noted  $r_1(t), \dots, r_N(t)$  and the energy is calculated as

$$E(r_0) = \sum_{j=1}^N \sum_{t=t_0}^{t_0+\Delta t} r_j(t)^2.$$

The singular values and the normalized energy are represented as a function of distance in decibel (Fig. 11). A clear enhancement at the target distance can be observed on those curves. The fact that several singular values increase might be explained by the presence of the boat, the anchor, the VRA, and probably by the fluctuations of the medium during acquisition. The backscattered energy after broadside transmission is higher after the target than before, this is explained by the slope change in the bottom profile that occurs near the target (see Figs. 2 and 13). Then the numerical back-

propagation in free space of the echo after broadside transmission is calculated [Fig. 12(a)]. A local maximum occurs at the height and range of the target but the greatest lobe occurs on the bottom ( $-4$  m) probably corresponding to the anchor maintaining the target. The energy spreading below, above, and just behind the target might be due to the presence of the boat and the VRA. Beyond the target, the focusing occurs on the bottom and the image of the bottom with respect to the surface, meaning that the broadside transmission produces strong reverberation after 140 m.

On the contrary, the backpropagation of the first singular vector focuses with good signal to noise ratio at the target and at its images with respect to the interfaces [Fig. 12(b)]. This confirms that it solely contains signal from the target. Around 130 m the singular vector mostly focuses on the image of the bottom with respect to the surface, meaning that the ray path with one reflection at the surface is the dominant one.

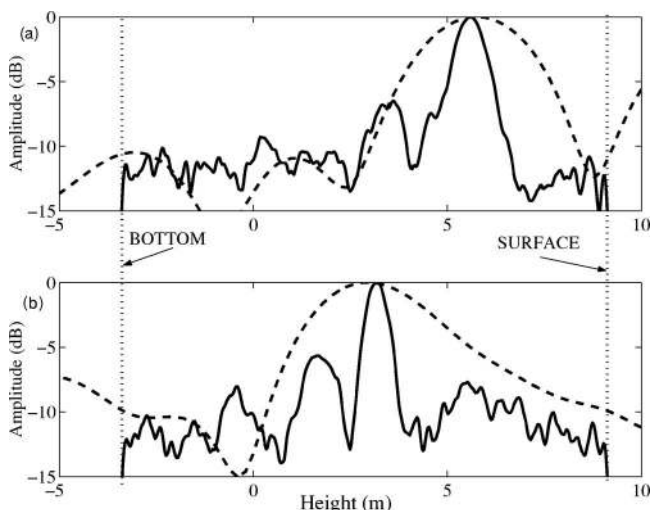


FIG. 10. Two targets at 253 m: Backpropagation of the first (a) and second (b) singular vectors calculated for  $r_0=253$  m in free space (dashed line) and using RAM (solid line).

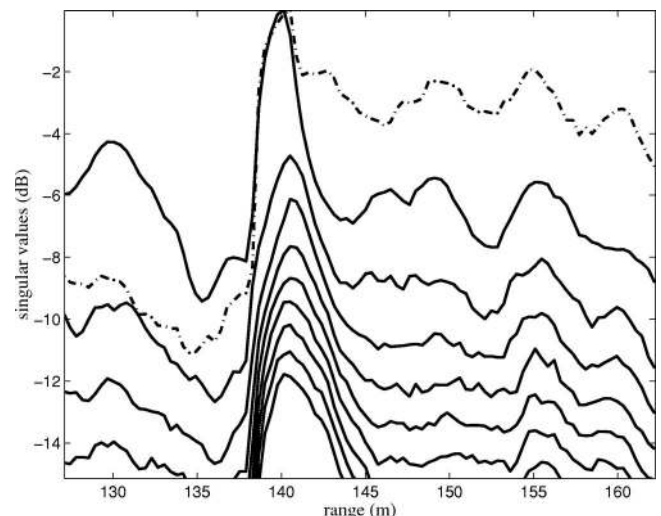


FIG. 11. One target at 143 m: Singular values as a function of distance (solid line) and normalized energy of the echo after broadside transmission (dash-dot) calculated for 3 ms shifted time windows.

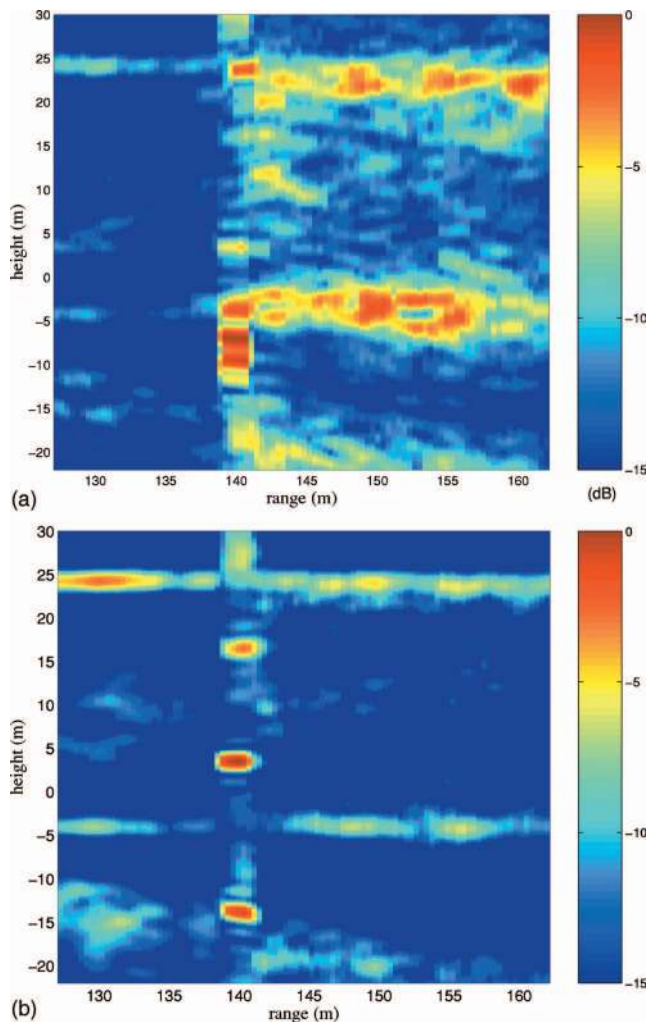


FIG. 12. One target at 143 m: Numerical backpropagation in free space of the echo after broadside transmission (a) and of the first singular vector (b) calculated for 3 ms shifted time windows.

### B. Backpropagation using RAM

To calculate the backpropagation with RAM, the array tilt is taken equal to  $2.9^\circ$  and the water depth at the array to

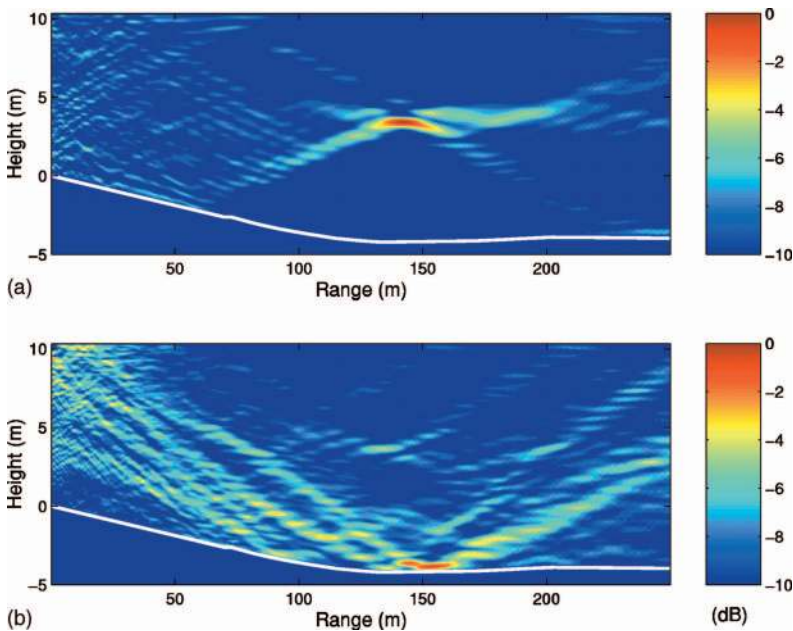


FIG. 13. One target at 143 m: Numerical backpropagation using RAM code of the first (a) and second (b) experimental singular vectors. Field are normalized and represented in decibel scale.

10.35 m. The first and second singular vectors are back-propagated over 250 m for several frequencies and the amplitude field is averaged (Fig. 13). The focusing clearly occurs at the target depth for the first singular vector, and the focal spot is about three times thinner than in free space as in the first experiment. The second singular vector focuses on the bottom, while some energy is also focused on the target (however 5 dB below). This might be explained by the fact that the target is not point-like ( $5 \lambda$ ) and probably moving around an average position.

### C. Active focusing with time reversal and DORT

The programmable parallel processed generators are used to time reverse the echo of the target. The VRA is deployed from the boat at the target distance and only eight elements spanning 3.5 m around the target are used to control the field. In the first stage, a time window is selected on the echo measured after broadside transmission, and the selected echo is time reversed. This transmission is repeated five times and each time, the transmitted signal is measured at the SRA (Fig. 14, left-hand side). The focusing occurs at height 3.8 m with significant secondary lobes. In the second stage, the first singular vector is calculated on the same time window at the central frequency. Then, this vector is transmitted to the SRA and the signal measured at the VRA (Fig. 14, right-hand side). As for time reversal, the transmission is repeated 5 times. Again, the maximum occurs at height 3.8 m, but with low secondary lobes.

In both cases, the focusing is achieved at the target. At this distance, the free space point spread function is about 1.7 m wide. In both cases, the main lobe is less than 1 m large, probably of the order of 50 cm, which means that more than two reflections (at bottom and surface) contribute to the focusing. For transmission of the singular vector, the secondary lobes are below 10 dB, which confirms the fact that the decomposition separates the echo of the target from the other contributions that can be attributed to the anchor, the VRA, the boat, or bottom reverberation. The strong tidal

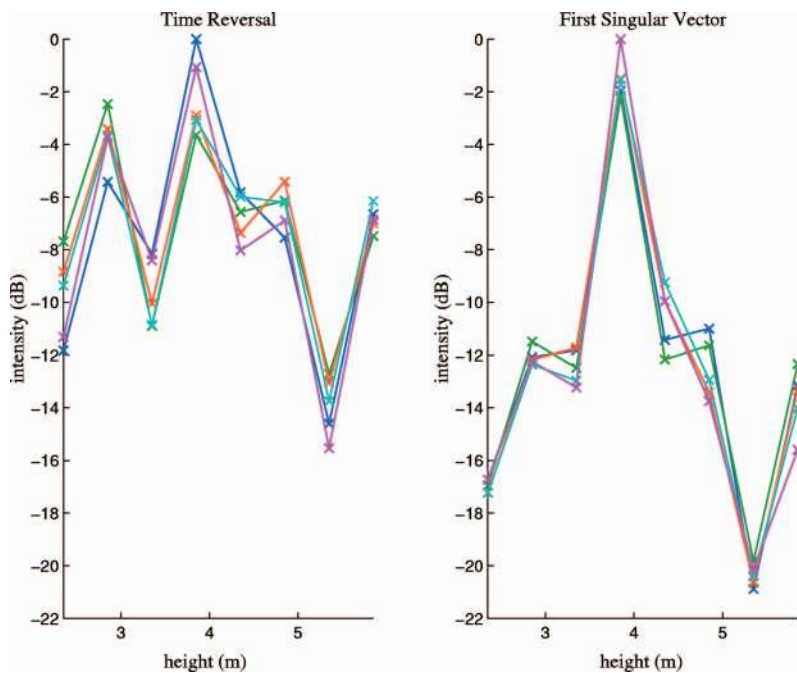


FIG. 14. One target at 143 m: Active focusing at the target using time reversal (left) and the first singular vector (right).

currents in the Bay of Brest made it difficult to deploy the vertical receiver array at longer distances. This is why the focusing experiment was done at a short range compared to the expected range of the system. Further experiments are required to determine the real limits of this system.

## VI. DISCUSSION

Detection experiments using the DORT method applied on data measured with a 24 elements vertical source-receiver array were presented. The experiments have been carried out in a reverberation limited shallow water environment using corner retroreflectors.

The results confirm those obtained in laboratory experiments. Two targets have been individually detected and correctly located within the water depth. The method appears to be robust and provides much better information on the target localization than conventional beam-forming on flat broadside transmissions.

In an experiment with a single target, active selective focusing by transmission of a singular vector has been shown to produce a strongly localized focal spot at the position of the scatterer. The obtained resolution was more than three times better than in free space. To the authors' knowledge, this is the first time that the DORT method was applied successfully to backscattered data in a real shallow water ocean environment with targets at range  $2500 \lambda$ , in depth  $100 \lambda$ . Beyond detection applications, this selective focusing ability also opens perspectives in underwater communication.

## ACKNOWLEDGMENTS

The authors are grateful to Dr Yann Stephan, from the French Hydrographic and Oceanographic Office, for providing the bathymetric model in the area. This work was funded by the French Armament Procurement Agency (DGA/SPN) under Contract No. 02 77 154 470 75 53.

Clorennec, D., de Rosny, J., Minonzio, J.-G., Prada, C., Fink, M., Folegot, T., Billand, P., Tavvry, S., Hibril, S., and Berniere, L. (2005). "First tests of the DORT method at 12 kHz in a shallow water waveguide," in Proceedings IEEE Oceans'05 Europe, Brest, France, Vol. 2, 1205–1209.

Collins, M. D., and Westwood, E. K. (1991). "A higher-order energy-conserving parabolic equation for range-dependent ocean depth, sound speed, and density," *J. Acoust. Soc. Am.* **89**, 1068–1075.

Edelmann, G., Akal, T., Hodgkiss, W., Kim, S., Kuperman, W., and Song, H. (2002). "An initial demonstration of underwater acoustic communication using time reversal," *IEEE J. Ocean. Eng.* **27**, 602–609.

Fink, M. (1997). "Time reversed acoustics," *Phys. Today* **50**, 34–40.

Folegot, T., Billand, P., Tavvry, S., Hibril, S., Berniere, L., de Rosny, J., Clorennec, D., Minonzio, J.-G., Prada, C., and Fink, M. (2005). "Design of a time reversal mirror for medium scale experiments," in Proceedings IEEE Oceans'05 Europe, Brest, France, Vol. 2, pp. 1210–1213.

Folegot, T., Prada, C., and Fink, M. (2003). "Resolution enhancement and separation of reverberation from target echo with the time reversal operator decomposition," *J. Acoust. Soc. Am.* **113**, 3155–3160.

Gaumond, C. F., Fromm, D. M., Lingeitch, J. F., Menis, R., Edelmann, G. F., Calvo, D. C., and Kim, E. (2006). "Demonstration at sea of the decomposition-of-the-time-reversal-operator technique," *J. Acoust. Soc. Am.* **119**, 976–990.

Kuperman, W. A., Hodgkiss, W. S., Song, H. C., Akal, T., Ferla, C., and Jackson, D. R. (1998). "Phase conjugation in the ocean: Experimental demonstration of an acoustic time-reversal mirror," *J. Acoust. Soc. Am.* **103**, 25–40.

Lingeitch, J. F., Song, H. C., and Kuperman, W. A. (2002). "Time reversed reverberation focusing in a waveguide," *J. Acoust. Soc. Am.* **111**, 2609–2614.

Mordant, N., Prada, C., and Fink, M. (1999). "Highly resolved detection and selective focusing in a waveguide using the DORT method," *J. Acoust. Soc. Am.* **105**, 2634–2642.

Prada, C., and Fink, M. (1994). "Eigenmodes of the time reversal operator: A solution to selective focussing in multiple target media," *Wave Motion* **20**, 151–163.

Sabra, K. G., Roux, P., Song, H.-C., Hodgkiss, W. S., Kuperman, W. A., Akal, T., and Stevenson, J. M. (2006). "Experimental demonstration of iterative time-reversed reverberation focusing in a rough waveguide application to target detection," *J. Acoust. Soc. Am.* **120**, 1305–1314.

Yokoyama, T., Kikuchi, T., Tsuchiya, T., and Hasegawa, A. (2001). "Detection and selective focusing on scatterers using the decomposition of time reversal operator method in Pekeris waveguide model," *Jpn. J. Appl. Phys., Part 1* **40**, 3822–3828.